University of Zurich[UZH]

Zurich Open Repository and Archive
University of Zurich
University Library
Strickhofstrasse 39
CH-8057 Zurich
www.zora.uzh.ch

Year: 2017

The autophagy machinery restrains iNKT cell activation through CD1D1 internalization

Keller, Christian W ; Loi, Monica ; Ewert, Svenja ; Quast, Isaak ; Theiler, Romina ; Gannagé, Monique ; Münz, Christian ; De Libero, Gennaro ; Freigang, Stefan ; Lünemann, Jan D

Abstract: Invariant natural killer T (iNKT) cells are innate T cells with powerful immune regulatory functions that recognize glycolipid antigens presented by the CD1D protein. While iNKT cell-activating glycolipids are currently being explored for their efficacy to improve immunotherapy against infectious diseases and cancer, little is known about the mechanisms that control CD1D antigen presentation and iNKT cell activation in vivo. CD1D molecules survey endocytic pathways to bind lipid antigens in MHC class II-containing compartments (MIICs) before recycling to the plasma membrane. Autophagosomes intersect with MIICs and autophagy-related proteins are known to support antigen loading for increased CD4+ T cell immunity. Here, we report that mice with dendritic cell (DC)-specific deletion of the essential autophagy gene Atg5 showed better CD1D1-restricted glycolipid presentation in vivo. These effects led to enhanced iNKT cell cytokine production upon antigen recognition and lower bacterial loads during Sphingomonas paucimobilis infection. Enhanced iNKT cell activation was independent of receptor-mediated glycolipid uptake or costimulatory signals. Instead, loss of Atg5 in DCs impaired clathrin-dependent internalization of CD1D1 molecules via the adaptor protein complex 2 (AP2) and, thus, increased surface expression of stimulatory CD1D1-glycolipid complexes. These findings indicate that the autophagic machinery assists in the recruitment of AP2 to CD1D1 molecules resulting in attenuated iNKT cell activation, in contrast to the supporting role of macroautophagy in CD4+ T cell stimulation.

DOI: https://doi.org/10.1080/15548627.2017.1297907

Posted at the Zurich Open Repository and Archive, University of Zurich
ZORA URL: https://doi.org/10.5167/uzh-147975
Journal Article
Accepted Version

Originally published at:
Keller, Christian W; Loi, Monica; Ewert, Svenja; Quast, Isaak; Theiler, Romina; Gannagé, Monique; Münz, Christian; De Libero, Gennaro; Freigang, Stefan; Lünemann, Jan D (2017). The autophagy machinery restrains iNKT cell activation through CD1D1 internalization. Autophagy, 13(6):1025-1036.
DOI: https://doi.org/10.1080/15548627.2017.1297907

The autophagy machinery restrains iNKT cell activation through CD1d internalization

Christian W. Keller,[1] Monica Loi,[2] Svenja Ewert,[3] Isaak Quast,[1,4] Romina Theiler,[3] Monique Gannagé,[5,6] Christian Münz,[2] Gennaro De Libero,[7,8*] Stefan Freigang,[3*] and Jan D. Lünemann[1*]

[1]Institute of Experimental Immunology, Laboratory of Neuroinflammation, University of Zurich, Zurich, Switzerland
[2]Institute of Experimental Immunology, Laboratory of Viral Immunobiology, University of Zurich, Zurich, Switzerland
[3]Institute of Pathology, Laboratory of Immunopathology, University of Bern, Bern, Switzerland
[4]Department of Immunology & Pathology, Monash University, Prahran, Australia
[5]Department of Pathology and Immunology, School of Medicine – CMU, University of Geneva, Geneva, Switzerland
[6]Division of Rheumatology, Department of Internal Medicine, University Hospital, Geneva, Geneva, Switzerland
[7]Singapore Immunology Network, Agency for Science, Technology and Research (A*STAR), Singapore, Singapore
[8]Department of Biomedicine, Laboratory of Experimental Immunology, University Hospital Basel, University of Basel, Basel, Switzerland

* equally contributing senior authors

Corresponding author: Jan D. Lünemann, Institute of Experimental Immunology, Laboratory of Neuroinflammation, University of Zurich, Winterthurerstrasse 190, CH-8057 Zurich, Switzerland, Phone: +41-44-635-3710, Fax: 212-327-7887, Email: jan.luenemann@uzh.ch

Text (Number of words): 5364

Abstract (Number of words): 217

Number of Figures: 5

Number of References: 58

Keywords: antigen presentation, autophagy, CD1d, dendritic cells, glycolipid, innate-like lymphocytes, internalization, NKT cell, T cell

Abstract

Invariant natural killer T (iNKT) cells are innate T cells with powerful immune regulatory functions that recognize glycolipid antigens presented by the CD1d protein. While iNKT-cell-activating glycolipids are currently being explored for their efficacy to improve immunotherapy against infectious diseases and cancer, little is known about the mechanisms that control CD1d antigen presentation and iNKT cell activation *in vivo*. CD1d molecules survey endocytic pathways to bind lipid antigens in MHC class II containing compartments (MIICs) before recycling to the plasma membrane. Autophagosomes intersect with MIICs and autophagy-related proteins are known to support antigen loading for increased $CD4^+$ T cell immunity. Here, we report that mice with DC-specific deletion of the essential autophagy gene *Atg5* showed better CD1d-restricted glycolipid presentation *in vivo*. These effects led to enhanced iNKT cell cytokine production upon antigen recognition and lower bacterial loads during *Sphingomonas paucimobilis* infection. Enhanced iNKT cell activation was independent of receptor-mediated glycolipid uptake or costimulatory signals. Instead, loss of *Atg5* in DCs impaired clathrin-dependent internalization of CD1d molecules via the adaptor protein complex 2 (AP2) and, thus, increased surface expression of stimulatory CD1d:glycolipid complexes. These findings indicate that the autophagic machinery assists in the recruitment of AP2 to CD1d molecules resulting in attenuated iNKT cell activation, in contrast to the supporting role of macroautophagy in $CD4^+$ T cell stimulation.

Introduction

Invariant natural killer T (iNKT) cells constitute a subset of T cells that expresses a semi-invariant TCR α chain (Vα24Jα18 in humans and Vα14Jα18 in mice) and recognize glycolipid antigens in the context of the MHC class I-related glycoprotein CD1d.[1] Upon TCR ligation, iNKT cells rapidly secrete large amounts of cytokines, such as IFNG and IL4, and act as an amplification relay at the interface of innate and adaptive immunity.[2] Due to their capacity to induce maturation of dendritic cells (DCs) for the initiation and maintenance of adaptive immune responses,[3-5] iNKT cells are regarded as a „natural adjuvant"; and iNKT cell agonists such α-galactosylceramide (αGalCer) and its analogues are currently being investigated in clinical trials as part of improved vaccination strategies against infections and cancers.[6] The mechanisms controlling lipid antigen loading onto CD1d molecules for iNKT cell activation are incompletely understood. After assembly in the endoplasmic reticulum, CD1 molecules follow the secretory pathway through the Golgi apparatus to the plasma membrane. Some CD1d molecules also associate with MHC class II molecules and the invariant chain, which directs CD1d complexes to endosomal compartments without first reaching the plasma membrane.[7,8] After trafficking to the plasma membrane, CD1 molecules including CD1d are internalized in order to sample antigens in the endo/lysosomal system[9] and, similar to MHC class II molecules,[10] recycle to the cell surface and present bound antigens to iNKT cells. Macroautophagy is an evolutionary conserved mechanism that delivers cytoplasmic constituents and substrates for MHC class II presentation to lysosomes and late endosomes.[11,12] Involvement of autophagy-facilitated transport is confirmed by studies using mice with DC-specific deletion of the essential autophagy gene *Atg5* that showed impaired $CD4^+$ T cell priming after herpes simplex virus infection.[12] Furthermore, human *Atg5*-deficient macrophages showed inefficient MHC class II presentation of extracellular antigens and decreased $CD4^+$ T cell stimulation.[13] The relevance of the autophagy machinery in lipid antigen loading within endosomal compartments has not received adequate attention. Here, we investigated its role in dendritic cell-mediated iNKT cell activation.

Results

Loss of *Atg5* increases the iNKT cell stimulatory capacity of dendritic cells

To investigate whether macroautophagy regulates CD1d trafficking, we initially determined the colocalization of CD1d with the microtubule-associated protein 1A/1B light chain 3 (LC3), present both on autophagosomes and LC3-associated phagosomes.[13,14] In sorted primary splenic DCs, LC3 and CD1d colocalized in steady state as determined by Pearson's correlation coefficient analysis. Activation of DCs with the toll-like receptor 9 agonist CpG, which facilitates DC-mediated iNKT cell activation,[15] significantly increased this colocalization (Fig. 1A). To test whether absence of the essential macroautophagy gene *Atg5* in DCs inhibits CD1d antigen presentation similar to MHC class II presentation,[13,16,17] we generated mice with conditional deletion of *Atg5* in DCs (*Atg5*$^{f/f}$ × CD11c-Cre, designated Cre^{+} *Atg5*$^{f/f}$). FACS-sorted splenic DCs isolated from Cre^{+} *Atg5*$^{f/f}$ mice and Cre^{-} *Atg5*$^{f/f}$ littermates were pulsed with different amounts of the prototypic iNKT agonist αGalCer and used to stimulate the iNKT cell hybridomas A.407 and FF13. Surprisingly, *Atg5*-deficient DCs were more potent in eliciting IL2 production by both iNKT cell lines (Fig. 1B, C). Conversely, induction of the autophagy machinery in wild type DCs by non-cytotoxic concentrations of the mTOR inhibitor rapamycin reduced IL2 production upon coculture with iNKT cells (Fig. 1D; Fig. S1). These data indicate that autophagy proteins in DCs may regulate iNKT cell responses.

To determine the mechanism of *Atg5*-dependent regulation of iNKT cell activation, we first evaluated whether Cre^{+} *Atg5*$^{f/f}$ DCs differed from Cre^{-} *Atg5*$^{f/f}$ DCs in their acquisition of lipid antigen. While the prototypic iNKT cell agonist αGalCer is taken up via both low density lipoprotein receptor (LDLR)-mediated and scavenger receptor-mediated pathways,[18] the nominal antigen digalactosylceramide (Galαgalcer) and the *Sphingomonas*-derived glucuronylceramide (GSL-1) require selective uptake via the LDLR or the scavenger receptor SRA, respectively.[18,19] The absence of *Atg5* in primary DCs resulted in more efficient stimulation of iNKT cell hybridomas independently of the type of antigen uptake, as shown by stimulation with LDLR-targeted (Galαgalcer), SRA-targeted (GSL-1), and

SRA/LDLR-targeted (αGalCer) glycolipid antigens (Fig. 2A). These findings suggest that the increased iNKT cell stimulation by *Atg5*-deficient DCs did not involve a unique type of internalizing receptor.

Our findings observed in primary DCs were unexpected and appeared to be in contrast with a recent study in which *Atg7*-deficient GM-CSF-differentiated bone marrow-derived DCs (BMDCs) did not differ from macroautophagy-competent BMDCs in eliciting cytokine production by iNKT cells.[20] To investigate this discrepancy we generated BMDCs from *Atg5*-deficient mice and also found that they elicit IL2 production by iNKT cells following uptake of glycolipid antigens to the same level as BMDCs from wild type mice (Fig. S2). Since *in vitro*-derived BMDC cultures contain heterogeneous cell populations including macrophages, DCs and neutrophils,[21,22] we additionally FACS-purified *in vitro* generated BMDCs for $CD11c^+$/MHC class II^+ cells which were subsequently loaded with increasing concentrations of αGalCer and co-incubated with iNKT cells. Increased IL2 production by iNKT cells were observed only in Cre^+ $Atg5^{f/f}$ $CD11c^+$/MHC class II^+ BMDC cultures loaded with high αGalCer concentrations (10 μg/ml) (Fig. S3). Even $CD11c^+$/MHC class II^+ BMDCs contain different myeloid cell subsets including common monocyte precursor-derived macrophages which are inferior to common DC precursor antigen-presenting cells in their T cell priming and stimulatory capacity.[22,23] We therefore continued to study DC-mediated iNKT cell activation using FACS-sorted primary splenic DCs. Next, we determined whether *Atg5*-deficient DCs differed from their *Atg5*-competent counterparts in providing costimulatory signals required for physiological iNKT cell activation, *i.e.* CD40 expression and IL12 production.[24] Cre^+ $Atg5^{f/f}$ DCs exhibited similar CD40 levels as Cre^- $Atg5^{f/f}$ DCs (Fig. 2B). Moreover, *Atg5*-deficiency did not affect the frequency of IL12-producing DCs or the total amount of IL12 secreted by DCs in response to CD40 ligation (Fig. 2C), in agreement with the reported unaltered expression levels of CD40 and CD86 as well as normal production of IL12p40, IL6 and TNF in *Atg5*-deficient DCs in the steady state.[12] Thus, loss of *Atg5* in DCs increases their capability for iNKT cell activation independently of receptor-mediated lipid targeting mechanisms and most costimulatory properties.

Increased CD1d surface expression in *Atg5*-deficient primary DCs

We next investigated whether loss of *Atg5* enhances the iNKT cell stimulatory capacity of DCs by affecting CD1d expression. We first determined CD1d surface expression levels in DCs compared to B cells derived from Cre^+ $Atg5^{f/f}$ mice and their Cre^- $Atg5^{f/f}$ littermates. Sorted $CD11c^+$/MHC class II^+ DCs and $CD19^+$/MHC class II^+ B cells were analyzed for CD1d expression (Fig. 3A). *Atg5*-deficient DCs showed significantly higher expression levels of surface CD1d protein (Fig. 3B), whereas no difference was observed for B cells which lacked Cre-expression and, thus, were autophagy-competent (Fig. S4A). To determine whether loss of *Atg5* regulates CD1d expression *in vivo*, Cre^+ $Atg5^{f/f}$ and Cre^- $Atg5^{f/f}$ mice were injected with αGalCer and CD1d presentation was investigated using the monoclonal antibody L363 that specifically detects CD1d:αGalCer-complexes, but does not bind to CD1d molecules loaded with other antigens.[25] Compared to autophagy-competent DCs, *Atg5*-deficient DCs showed increased expression levels of CD1d:glycolipid complexes (Fig. 3C). Levels of stimulatory CD1d:antigen complexes were similar for B cells in Cre^+ $Atg5^{f/f}$ mice (Fig. 3C). In contrast to CD1d, the expression levels of CD11c and MHC class II remained unchanged in Cre^+ $Atg5^{f/f}$ DCs (Fig. 3D).

Loss of *Atg5* impairs CD1d internalization but not CD1d recycling to the cell surface

CD1d expression levels at the cell surface are largely determined by the rates of CD1d internalization and recycling through endosomal and lysosomal compartments.[26,27] Therefore, we separately analyzed the rates of CD1d internalization and CD1d recycling to the cell surface in primary *Atg5*-deficient and wild type DCs. To evaluate the kinetics of CD1d internalization, we determined the remainder of previously biotin-labeled CD1d molecules at the cell surface by flow cytometry. To assess CD1d recycling rates, we quantified newly resurfaced CD1d molecules after the cell surface CD1d had been previously blocked with unconjugated anti-CD1d antibodies (Fig. 4A). CD1d internalization was significantly impaired (Fig. 4B), whereas trafficking of intracellular CD1d molecules back to the cell surface remained unaffected in Cre^+ $Atg5^{f/f}$ DCs (Fig. 4C). As expected, B cells derived from Cre^+ $Atg5^{f/f}$ mice and Cre^- $Atg5^{f/f}$ littermates

showed similar kinetics of CD1d turnover (Fig. 4B, C). Thus, loss of *Atg5* in primary DCs impairs CD1d internalization, leading to increased CD1d surface expression levels and an enhanced capacity of *Atg5*-deficient DCs to activate iNKT cells.

Reduced endosomal recruitment of CD1d and its adaptor protein AP2 in *Atg5*-deficient primary DCs

Internalization of murine CD1d (mCD1d), which contains a tyrosine-based endosomal-targeting motif in its cytoplasmic tail,[28] follows a clathrin-dependent pathway that allows binding of mCD1d to adaptor protein complexes (AP). Murine CD1d molecules bind AP2, which is expressed at the plasma membrane and targets internalized CD1d molecules to endosomal compartments.[29-31] During macroautophagy, LC3 conjugation to the autophagosomal membrane promotes recruitment of specific substrates into autophagosomes via LC3 binding anchor proteins which function as selective autophagy receptors in the presence of LC3-interacting regions (LIRs).[32,33] AP2 has previously been identified to contain a LIR motif within its α-subunit, and this LC3 binding by AP2 facilitates delivery of β-amyloid precursors for lysosomal degradation.[34] To determine whether loss of autophagy proteins impairs trafficking of AP2 and CD1d to endosomal compartments in primary DCs, colocalization of both molecules with the early endosomal antigen-1 (EEA1) was evaluated by confocal microscopy (Fig. 4D). Colocalization of AP2 and CD1d with EEA1 was significantly reduced in *Atg5*-deficient DCs as compared to Cre^{-} $Atg5^{f/f}$ DCs (Fig. 4E). These data suggest that autophagy proteins assist in the recruitment of CD1d molecules into endosomal compartments and provide a mechanistic explanation as to how loss of autophagy proteins stabilizes the cell surface expression of CD1d:glycolipid complexes on DCs.

Autophagy proteins in DCs regulate *i*NKT cell responses to lipid immunization and microbial infection *in vivo*

We investigated whether loss of *Atg5* regulates iNKT cell activation and DC maturation upon αGalCer challenge *in vivo*. Frequencies of iNKT cells, DCs and B cells were comparable in Cre^{+} $Atg5^{f/f}$ and Cre^{-} $Atg5^{f/f}$ mice at steady state (Fig. 5A, Fig. S4B).

Downregulation of the T cell receptor precluded the evaluation of iNKT cell frequencies and activation markers 12 hours after αGalCer challenge.[35] Therefore, we determined IFNG and IL4 serum levels after glycolipid challenge *in vivo*. Following αGalCer injection, Cre^{+} $Atg5^{f/f}$ mice showed substantially higher IL4 levels after 4 hours and IFNG levels after 12 hours, as compared to Cre^{-} $Atg5^{f/f}$ mice (Fig. 5B). αGalCer-mediated activation of iNKT cells leads to full DC maturation *in vivo* within 4 hours.[3] The increased and prolonged iNKT cell activation observed in Cre^{+} $Atg5^{f/f}$ mice was associated with enhanced phenotypic DC maturation as indicated by increased expression levels of CD86 as well as CD40 12 hours after αGalCer challenge while costimulatory molecule expression in B cells remained similar in αGalCer-treated Cre^{+} $Atg5^{f/f}$ and Cre^{-} $Atg5^{f/f}$ mice (Fig. 5C, Fig. S5).

We next investigated whether the enhanced iNKT cell stimulatory capacity of *Atg5*-deficient DCs as observed upon αGalCer-challenge conferred protection against infection with *Sphingomonas*. The gram-negative, lipopolysaccharide-free bacterium *Sphingomonas paucimobilis (S. paucimobilis)*, associated with opportunistic and nosocomial infections in immunocompromised patients,[36] is known to contain glycosphingolipids which stimulate iNKT cells through their TCR in a CD1d-specific manner.[37-40] Although the stimulatory potential of *S. paucimobilis*-derived glycosphingolipids is lower as compared to αGalCer, iNKT cell recognition of these natural microbial glycolipids induces proinflammatory cytokine production *in vitro* and *in vivo*.[37,39,41] Upon infection with *S. paucimobilis*, Cre^{+} $Atg5^{f/f}$ mice exhibited significantly lower pathogen loads in spleens and lungs as compared to their Cre^{-} $Atg5^{f/f}$ counterparts (Fig. 5D). Reduced pathogen loads were associated with increased serum levels of proinflammatory cytokines such as the IFNG-induced protein 10 (IP10) and TNF. Production of IFNG tended to be higher

in Cre^{+} *Atg5*$^{f/f}$ mice, whereas IL17 production was unchanged (Fig. 5D). Thus, autophagy proteins in DCs regulate surface expression of stimulatory CD1d:glycolipid complexes, shape iNKT cell activation and subsequent DC maturation in response to αGalCer and natural microbial glycolipids *in vivo.*

Discussion

The autophagic machinery enhances adaptive immunity by supporting antigen loading onto MHC class II molecules and is currently being explored for its potential to improve T cell responses upon vaccinations in order to establish long-lasting T cell memory.[42-45] Autophagosomes can fuse with MHC class II containing compartments and deliver intracellular antigens for loading onto MHC class II and MHC class I molecules.[44,46-48] In addition, autophagy regulates exogenous antigen processing through the LC3-phosphatidylethanolamine-conjugation machinery during LC3 associated phagocytosis, a process which requires *Atg5* and facilitates MHC class II loading.[12-14,17] Both pathways support loading of vesicular antigens onto MHC molecules, leading to increased and more efficient $CD4^{+}$ T cell responses. A fraction of CD1d proteins associates with MHC class II and invariant chain complexes which are sorted into late endosomal MIICs before trafficking to the cell surface[7,8] However, in contrast to the supportive activity on MHC class II presentation, we found that autophagy proteins negatively regulate the presentation of lipid antigens by CD1d. Loss of *Atg5* in DCs impaired CD1d internalization, leading to increased expression of stimulatory CD1d:glycolipid complexes and enhanced iNKT cell activation.

Internalization of CD1 molecules from the plasma membrane is essential for their ability to sample antigens in the endocytic system.[28,49] CD1d molecules are internalized in clathrin-coated pits via the interaction of AP2 and AP3 with tyrosine-based sorting motifs present in the cytoplasmic tails of CD1.[50,51] Tian et al. identified a LIR motif within the α-subunit of AP2 (AP2A1), which was reported to mediate enhanced Alzheimer precursor protein internalization and degradation.[34] Once this motif was mutated to alanine repeats, AP2A1 did not longer coimmunoprecipitate with LC3.[34] In line with this identification of AP2 as an LC3-interacting protein,[34] we found that loss of *Atg5* impairs trafficking of

both AP2 and CD1d molecules into endosomal compartments. Altogether, these data indicate that internalization of CD1d occurs less efficiently if AP2 cannot be recruited via LC3, leading to increased surface expression of stimulatory CD1d:glycolipid complexes.

Similar to CD1d, surface levels of classical MHC class I molecules were recently reported to be elevated due to decreased endocytosis and degradation.[52] However, AP2 components were not significantly reduced in immunoprecipitates of classical MHC class I molecules derived from *Atg5*-deficient cells compared to wild type counterparts. Instead, *Atg5*-deficiency compromised MHC class I association with the AP2-associated kinase 1 which can support AP2-independent, but clathrin-dependent endocytosis pathways.[52-54] Furthermore, LIR motifs have also been described in clathrin itself.[55] Thus, autophagy proteins appear to affect different clathrin-dependent pathways for the internalization and degradation of classical and non-classical MHC class I molecules, respectively.

Loss of autophagy proteins was recently reported to exert a T cell-intrinsic role in regulating iNKT cell development.[20,56] Mice with T lymphocyte-specific deletion of *Atg5* or *Atg7* show reduced progression of thymic iNKT cells through the cell cycle and lower frequencies of both thymic and peripheral iNKT cell populations due to increased apoptosis and impaired survival.[20,56] Frequencies of thymic and peripheral iNKT cells were unchanged in Cre^{+} $Atg5^{f/f}$ mice supporting the notion that the reported deficit in iNKT cell differentiation is cell-autonomous. Our data indicate that while autophagy proteins regulate iNKT cell development via T cell-intrinsic effects, they attenuate peripheral iNKT activation through their function in DC-mediated antigen processing and presentation.

In conclusion, our findings indicate that the autophagic machinery regulates iNKT cell responses through CD1d internalization. These data broaden the concept of *Atg*-mediated antigen presentation and indicate that autophagy-related proteins might not only enhance, as previously described with MHC class II-restricted presentation of peptide antigens, but also limit and tune the presentation of lipid antigens and the activation of innate T cells. Its function in tuning lipid antigen presentation could potentially limit the efficacy of vaccination strategies that include iNKT cell ligands as adjuvants and target macroautophagy for improved $CD4^{+}$ T cell immunity.[44,45] A clear and comprehensive concept of how the autophagy

machinery couples to antigen-presentation and lymphocyte activation appears to be required to predict the outcome of therapeutic interventions in this pathway to boost adaptive immunity.

Materials and Methods

Immunocytochemistry and colocalization assays

For assessing colocalization between LC3/CD1d, CD1d/EEA1 or AP2/EEA1 in splenic DCs, C57BL/6-, Cre^+ $Atg5^{f/f}$- or Cre^- $Atg5^{f/f}$-derived splenocytes were MACS-sorted via magnetic CD11c microbeads (Miltenyi Biotech, 130-097-059) according to the manufacturer's recommendation using an autoMACS Pro separator (Miltenyi Biotech, 130-092-545). MACS-purified $CD11c^+$ cells were plated out in 0.01% poly-l-lysine (Sigma-Aldrich, P4707-50ML) in ddH_2O pretreated 8-well glass chamber slides (Nunc Lab-Tek, NUNC-177402) at 1×10^5/chamber. For assessing colocalization between LC3/CD1d, $CD11c^+$ splenocytes were then either kept in R10 (RPMI-1640 (Life Technologies, 7001612) + 10% FCS (Sigma-Aldrich, F2442-6X500ML) + 50 U/ml P/S (Life Technologies, 15070-063) only or R10 supplemented with 2 μg/ml of the B-class murine toll-like receptor 9 agonist CpG ODN 1826 (InvivoGen, tlrl-1826-5) for 5 hours at 37° C and 5% CO_2. A cytospin was performed (3 min, 300 g), supernatants were carefully aspired and chambers were washed twice (200 μl/chamber) with cold phosphate buffered saline (PBS; Thermo Fisher Scientific, 10010023). Cells were fixed for 15 min at room temperature (RT) in 3% paraformaldehyde (PFA; Santa Cruz Biotechnology, sc-281692) in PBS followed by two washing steps with PBS (200 μl/chamber). For CD1d/EEA1 colocalization studies, cells were incubated with Fc receptor III/II blocking antibody, labeled for CD1d 30 min at 4° C, then incubated at 37° C for an additional hour in R10, before fixation. Cells were permeabilized for 5 min at RT in 200 μl of 0.1% Triton X-100 (Sigma-Aldrich, X100-500ML) in PBS followed by 30 min of blocking with 100 μl of 1% bovine serum albumin (Sigma-Aldrich, A9576-50ML) /10% normal goat serum (NGS; Sigma-Aldrich, G9023-5ML) in PBS at RT. Afterwards cells were incubated with primary antibodies (rabbit-anti-LC3, rat-anti-CD1d, goat anti-EEA1, mouse-anti-AP2) in 0.1% saponin (Sigma-Aldrich, 47036-50G-F) /10%

NGS in PBS for 1 hour at RT. Chambers were carefully washed twice with 0.1% saponin in PBS (200 µl/chamber) followed by a 45 min incubation with secondary antibodies in 0.1% saponin/10% NGS in PBS (Alexa488-conjugated or Alexa555-conjugated anti-rabbit, anti-rat, anti-goat, and anti-mouse). Cells were washed twice with PBS (200 µl/chamber), followed by incubation with 4',6-Diamidino-2-Phenylindole, Dihydrochloride (Thermo Fisher Scientific, D1306) for 2 min at RT. Washing steps as above were performed and slides were mounted with ProLong Gold antifade mountant (Thermo Fisher Scientific, P36930), let sit for 24 hours at RT in the dark and were then transferred to 4° C in the dark until further analysis. Pictures were acquired using a 63×, 1.4 NA oil immersion lens with an inverted confocal laser scanning microscope (Leica SP5-UV). To determine colocalization, Pearson's correlation coefficient values were calculated using JACoP (Just Another Colocalization Plugin) in ImageJ software. A Pearson score >0.6 indicates a statistically relevant colocalization of the signals.

Coculture assays with splenic DCs

CD1d-mediated presentation of lipid antigens was measured using the murine Vα14$^+$/Vβ8$^+$ iNKT cell hybridomas A.407 and FF13. NKT cell hybridomas were cultured in hybridoma culture medium (RPMI-1640 supplemented with 10% FCS, 50 U/ml P/S, 2 mM L-glutamine (Thermo Fisher Scientific, 25030081) and non-essential amino acids (Thermo Fisher Scientific, 11140050) at 37° C and 5% CO_2. For coculture assays Cre$^-$ *Atg5$^{f/f}$*- and Cre$^+$ *Atg5$^{f/f}$*-derived splenocytes were purified for CD11c$^+$ cells using magnetic microbeads according to the manufacturer's recommendation. CD11c-enriched fractions were further purified through FAC-sorting using an ARIA III FCF (gated on live CD11c/I-A^b double-positive cells). Purified splenic DCs were directly sorted in round-bottom 96-well tissue culture plates at 3×10^4 cells/well and kept in R10 at 37° C and 5% CO_2 for 45 min in order to settle. Afterwards, wells were either supplemented with increasing amounts of the glycolipid antigen αGalCer (0.01 - 10 µg/ml) or left untreated for 4 hours. Each condition was applied in triplicates. Wells were carefully washed 3×

with PBS (200 µl/well) and 5×10^4 NKT hybridoma cells (A.407 or FF13) in hybridoma culture medium were added to a final volume of 200 µl/well. Control wells containing antigen-presenting cells- and iNKT hybridoma cells-only (with or without addition of αGalCer) were included. Wells were incubated at 37° C and 5% CO_2. After 24 hours cell culture supernatants were collected for analysis of IL2 concentrations via ELISA. In some experiments titrated concentrations of indicated glycolipid antigens were used instead of αGalCer.[18]

Coculture assays with BMDCs

BMDCs were generated by culturing the bone marrow of Cre^- *Atg5*$^{f/f}$ or Cre^+ *Atg5*$^{f/f}$ mice in presence of 2 ng/ml recombinant GM-CSF (Biolegend, 576306) *in vitro*. After 7 days, differentiated BMDCs were harvested, purified over a 14.5% Histodenz (Sigma-Aldrich, D2158-100G) gradient and pulsed with titrated amounts of lipid antigens for 4 hours at 37° C and 5% CO_2. Cells were then washed, and 1×10^4 BMDCs were used to stimulate 5×10^4 A.407 iNKT hybridoma cells in triplicate cultures in 96-well tissue culture plates. IL2 concentrations in 24 hours cell culture supernatant were determined by ELISA. In some experiments, BMDCs were further purified via FAC-sorting for $CD11c^+$/ $I\text{-}A^{b+}$ cells.

Flow cytometry

For surface expression analysis of CD40, CD1d, CD11c and $I\text{-}A^b$, Cre^- *Atg5*$^{f/f}$- and Cre^+ *Atg5*$^{f/f}$-derived splenocytes were purified for $CD11c^+$ cells using magnetic microbeads according to the manufacturer's recommendation. After Fc receptor block (22.4 µg/ml, 20 min, 4° C) and subsequent washing step, CD11c-enriched fractions were stained for 20 min with LIVE/DEAD fixable Aqua Dead stain kit (Thermo Fisher Scientific, L34957) in PBS at 4° C in the dark. The CD11c-depleted fractions were used for CD1d surface stainings of B cells (gated on CD19/$I\text{-}A^b$ double-positive cells). Samples were washed twice in cold PBS followed by incubation with respective fluorochrome-labeled antibodies in FACS

buffer (1% bovine serum albumin/0.1% NaN_3 (Sigma-Aldrich, S8032-500G) in PBS) for 25 min at 4° C in the dark. After 2 washing steps with cold PBS samples were resuspended in 50 µl of FACS buffer prior to sample acquisition using a BD FACSCanto-II. For IL12 intracellular cytokine staining (ICS) using a Fixation/Permeabilization Solution Kit (eBioscience, 88-8824-00), CD11c-enriched fractions were plated out at 5×10^5 cells/well in 48-well tissue culture plates and incubated for 12 hours in R10 either supplemented with 15 µg/ml anti-CD40 or not at 37° C and 5% CO_2. For flow cytometry analysis of $IL12^+$ cells, samples were additionally treated with Brefeldin A (Sigma-Aldrich, B5936-200UL; used at 10 µg/ml) during the last 5 hours of incubation to block IL12 secretion. Cells were washed twice with PBS and stained for live cells and the surface molecules CD11c and $I\text{-}A^b$ (see above). Fixation and permeabilization for subsequent ICS were carried out according to the manufacturers recommendations (Fixation/Permeabilization Solution Kit). Samples were acquired with a BD FACSCanto-II and all data were analyzed using FlowJo software (Tree Star Inc.). The same set up as the ICS experiments was carried out omitting the addition of Brefeldin A. In these instances, cell culture supernatants were collected after 12 hours for analysis of secreted IL12 via ELISA.

iNKT cell detection

iNKT cells were detected using αGalCer-loaded CD1d tetramers. Single-cell suspensions from spleens, livers, and thymi were pre-treated with Fc Block and 0.5 mg/ml avidin (Sigma-Aldrich, A9275-1MG) in FACS buffer for 10 min. After 2 washes, cells were incubated with CD1d/αGalCer tetramers at RT for 15 min before addition of anti-CD3ε and further staining for 30 minutes. Washed cells were then depleted of erythrocytes, fixed with BD FACS Lysing Solution (BD Biosciences, 349202), and acquired on a BD LSR II using FACSDiva software. Analysis was performed using the FlowJo software (Tree Star Inc.).

Determination of cytokine concentration

IL2 concentration in coculture supernatants was measured using a Mouse IL2 Ready-SET-GO reagent kit (eBioscience, 88-7024-76). IL12 concentration in cell culture supernatants was measured using the Mabtech Mouse IL12/IL23 p40 ELISA development kit (Mabtech, 3451-1H-6). Serum concentrations of IFNG and IL4 were measured using the Mouse IFNG or Mouse IL4 Instant ELISA kit (eBioscience, BMS606INST and BMS613INST). All measurements were carried out according to the respective manufacturer's recommendation.

Mice

8 to 12 weeks old C57BL/6 (Janvier), *Atg5*$^{flox/flox}$,[57] Tg(Itgax-cre,-EGFP)4097Ach designated CD11c-Cre (Jackson), were bred and housed in the University of Zurich animal facility in individually ventilated cages according to Swiss animal laws and institutional guidelines. *Atg5*$^{flox/flox}$ mice were crossed to CD11c-Cre mice to obtain CD11c-Cre × *Atg5*$^{flox/flox}$ mice (designated Cre^{+} *Atg5*$^{f/f}$) on a C57BL/6 background. *Atg5*$^{flox/flox}$ mice (designated Cre^{-} *Atg5*$^{f/f}$) were used as littermate controls. All animal protocols were approved by the cantonal veterinary office of the canton of Zurich, Switzerland (protocol 25706-ZH209/2014) and the canton of Bern, Switzerland (protocols BE46/14, BE73/14).

Genotyping

Animal genotype was confirmed by PCR analysis on DNA from tail or ear biopsies by the use of the following primer pairs (5'-3'):

Atg5$^{flox/flox}$	GAATATGAAGGCACACCCCTGAAATG
Atg5$^{flox/flox}$	GTACTGCATAATGGTTTAACTCTTGC
Atg5$^{flox/flox}$	ACAACGTCGAGCACAGCTGCGCAAGG
Atg5$^{flox/flox}$	CAGGGAATGGTGTCTCCCAC
CD11c-Cre	GCGGTCTGGCAGTAAAAACTATC

CD11c-Cre GTGAAACAGCATTGCTGTCACTT

CD11c-Cre CTAGGCCACAGAATTGAAAGATCT

CD11c-Cre GTAGGTGGAAATTCTAGCATCATCC

Mouse organ processing

After mice were euthanized with CO_2, spleens were removed, collected in cold PBS, dissected into small pieces and digested for 30 min at 37° C and 5% CO_2 with Collagenase D (Sigma-Aldrich, 000000011088866001; used at 0.4 mg/ml) and DNAse (Qiagen, 79254; used at μg/ml) in PBS. Digest was stopped with EDTA (Sigma-Aldrich, ED-500G; used at 10 mM) for 5 min at 37° C and 5% CO_2. The digested tissue was passed through a 70-μm cell strainer (Fisher Scientific, 08-771-2) to obtain single cell solutions. After washing step with cold PBS a red blood cell lysis (2 min, RT) was performed using 1 ml/spleen ACK lysis buffer (Thermo Fisher Scientific, A1049201) followed by washing with cold PBS. Single cell solutions were kept on ice until further processing.

CD1d internalization assay

For assessing internalization of surface CD1d in splenic DCs and B cells respectively, Cre^{-} *Atg5*$^{f/f}$ - and Cre^{+} *Atg5*$^{f/f}$ -derived splenocytes were purified for $CD11c^{+}$ cells using magnetic microbeads according to the manufacturer's recommendation. After Fc receptor block (22.4 μg/ml, 20 min, 4° C) and subsequent washing step, the CD11c-enriched fraction was incubated for 30 min on ice with a biotinylated-CD1d antibody. After extensive washing with ice cold PBS cells were fractionated into the following groups (1×10^5/group): 90 min on ice, 90, 60 and 30 min at 37° C, 5% CO_2. To assess CD1d internalization in B cells, the negative fraction from the MACS purification was processed accordingly in parallel. After respective incubation time, cells were washed with ice cold PBS and incubated with PE-labeled streptavidin, anti-CD11c (CD11c-enriched fraction for DC analysis) or anti-CD19 (CD11c-depleted fraction for B cell analysis), anti-I-A^b and LIVE/DEAD fixable Aqua Dead stain kit for 20 min

on ice in the dark. Samples were fixed with 3% PFA in PBS and acquired with a BD FACSCanto-II. All data were analyzed using FlowJo software (Tree Star Inc.). To obtain *% internalized CD1d* values, the following equation was employed:

$$\%\ \text{internalized CD1d} = 100 - [\left(\frac{\text{MFI sample}}{\text{MFI 90 min ice}}\right) \times 100]$$

CD1d recycling assay

CD11c-enriched or -depleted fractions of Cre^- *Atg5*$^{f/f}$- and Cre^+ *Atg5*$^{f/f}$-derived splenocytes (see internalization assay for details) were incubated with protein synthesis inhibitor cycloheximide (Sigma-Aldrich, 01810-1G; used at 1 μg/ml) supplemented R10 (60 min at 37° C, 5% CO_2). After extensive washing with ice cold PBS, cells were either incubated with unconjugated anti-CD1d antibody for 30 min (pre-blocked) or left untreated (non-blocked) on ice. After washing step, cells were divided into the following groups (1×10^5/group): 30 min on ice (pre-blocked), 30 min on ice (non-blocked), 30, 20, 10, 5 min at 37° C, 5% CO_2. After respective incubation times, cells were washed with ice cold PBS and incubated with PE-labeled anti-CD1d antibody (of the same clone used for pre-blocking), anti-CD11c (CD11c-enriched fraction for DC analysis) or anti-CD19 (CD11c-depleted fraction for B cell analysis), anti-I-A^b and LIVE/DEAD fixable Aqua Dead stain kit for 20 min on ice in the dark. A non-blocked sample was stained with PE-labeled isotype control instead of the PE-labeled anti-CD1d antibody. Samples were fixed with 3% PFA in PBS and acquired with a BD FACSCanto-II. All data were analyzed using FlowJo software (Tree Star Inc). To obtain *% recycled CD1d* values, the following equation was employed:

$$\%\ \text{recycled CD1d} = [\frac{(\text{MFI sample} - \text{MFI preblocked})}{(\text{MFI unblocked AB} - \text{MFI unblocked isotype})}] \times 100.$$

Lipid *in vivo* chase

Cre^- $Atg5^{f/f}$ and Cre^+ $Atg5^{f/f}$ mice were either injected intraperitoneally (i.p.) with 200 μl PBS or α GalCer (1 μg). Injection time points were chosen as such that animals could be sacrificed at the same time point. Blood for serum cytokine analysis was collected via cardiac puncture. Blood was utilized for serum cytokine analysis (IFNG, IL4). Spleens were processed as described above (see mouse organ processing). MFI of co-stimulatory molecules was analyzed on either Cre^+ (Cre^+ $Atg5^{f/f}$) or Cre^- (Cre^- $Atg5^{f/f}$) CD11c/I-A^{b+} splenocytes.

Infection with *S. paucimobilis*

Mice were intravenously (i.v.) infected with 10^7 colony forming units (CFU) *S. paucimobilis* (ATCC, 29873) and organs were harvested and weighed at 24 hours post infection. After smashing organs in sterile H_2O using a tissue lyzer (Qiagen, 85300), tenfold serial dilutions were plated onto Muller-Hinton agar (Sigma-Aldrich, 70192) containing 200 μg /ml streptomycin (Sigma-Aldrich, S9137) and incubated for 48 hours at 30° C. Colonies were then counted and bacterial titers calculated as CFU per g tissue.

Statistics

Statistical significance was determined using the unpaired two-tailed T test and Mann-Whitney U test in Prism software (GraphPad Software Inc.). $P < 0.05$ was considered significant.

Antibodies, streptavidin, tetramer and iNKT lipid agonists

Unconjugated anti-murine CD40 (Bio X Cell, BE0016-2; clone: FGK4.5/ FGK45), unconjugated anti-murine CD16/32 (Bio X Cell, CUS-HB-197; clone 2.4G2), PE-conjugated anti-murine CD1d (eBioscience, 12-0011-83; clone: 1B1), PE-conjugated rat IgG2bκ□□eBioscience, 12-4031-83; □□□□□□□□□□□□□□□□□□□□, PE-conjugated anti-α-GalCer:CD1d-complex (eBioscience, 12-2019-82; clone: L363), PE-conjugated anti-murine IL12/IL23 p40 (eBioscience, 12-7123-81; clone:

C17.8), PerCP-Cy5.5-conjugated anti-murine CD8 (eBioscience, 45-0081-82; clone: 53.6.7), unconjugated anti-murine CD1d (Biolegend, 123515; clone: 1B1), biotinylated anti-murine CD1d (Biolegend, 123506; clone: 1B1), Pacific Blue-conjugated anti-murine CD19 (Biolegend, 115523; clone: 6D5), Pacific Blue-conjugated anti-murine CD4 (Biolegend, 100428; clone: GK1.5), PE-conjugated anti-murine CD40 (Biolegend, 124610; clone: 3/23), PE-Cy7-conjugated anti-murine CD11c (Biolegend, 117318; clone: N418), APC-conjugated anti-murine I-A^b (clone: Biolegend, 107614; M5/114.15.2), APC-conjugated anti-murine CD3 (Biolegend, 100236; clone: 17A2), PE-conjugated streptavidin (Biolegend, 405204), unconjugated anti-LC3 (MBL International Corporation, PM036), Alexa Fluor488-conjugated F(ab')2-goat anti-rabbit IgG (H+L) (Thermo Fisher Scientific, A-11070) or -donkey anti-goat IgG (H+L) (Thermo Fisher Scientific, A-11055) and Alexa Fluor555-conjugated F(ab')2-goat anti-rat (H+L) (Thermo Fisher Scientific, A-21434) or -rabbit anti-mouse IgG (H+L) (Thermo Fisher Scientific, A-21427), unconjugated anti-EEA1 (Antibodies-online, ABIN1439993), unconjugated anti-AP2 (BD Biosciences, 610502; clone 8/Adaptin alpha), PE-conjugated αGalCer-loaded CD1d tetramer (ProImmune, E001-2A), αGalCer (Adipogen, AG-CN2-0013-M001), GSL-1 and GalαGalCer (Avanti Polar Lipids, Inc.)

iNKT cell hybridoma lines

The $V\alpha14^+/V\beta8^+$ iNKT cell hybridoma A.407 was generated by fusion of *ex vivo* CD1d tetramer-sorted iNKT cells with the murine thymoma BW5147 (S.F. unpublished data). The FF13 hybridoma was generated by fusion of Vα14 iNKT cells sorted from αGalCer-treated C57BL/6 mice with mouse BW5147 thymic lymphoma cells. [58]

Abbreviations

αGalCer	α-galactosylceramide
AP2	adaptor protein complex 2
Atg	autophagy related gene
BMDC	bone marrow-derived DC
DC	dendritic cell
EEA1	early endosome antigen 1
Galαgalcer	digalactosylceramide
GM-CSF	granulocyte-macrophage colony-stimulating factor
GSL-1	glucuronylceramide
IFN	interferon
IL	interleukin
iNKT	invariant natural killer T cell
IP10	IFNG-inducible protein 10
LC3	microtubule-associated protein 1A/1B light chain 3
LDLR	low-density lipoprotein receptor
LIR	LC3-interacting region
MIIC	MHC class II loading compartment
MHC	major histocompatibility complex
S. paucimobilis	*sphingomonas paucimobilis*
SRA	scavenger receptor A
TCR	T cell receptor
TNF	tumor necrosis factor

Acknowledgements

C.W.K. was supported by a scholarship provided by the German Research Foundation (DFG grant KE 1831/1-1 to C.W.K). This work was supported by grants of the Dürmüller-Bol-Stiftung, Uni-Bern-Forschungsstiftung and the Vontobel-Stiftung (to S.F.), EU HORIZON 2020 project "TBVAC 2020" (grant 643381), the Swiss National Foundation (310030-149571), the EU HORIZON 2020 project "TBVAC 2020" (grant 643381), the BMRC-SERC Diagnostic grant call 1121480006, and A*STAR Singapore/Australian NHMRC (1201826277) (to G.D.L.). J.D.L.was supported by the Swiss National Foundation (31003A-169664), the Novartis Foundation for medical-biological research, the Sassella Foundation, the Hartmann Müller Foundation, and the Swiss Multiple Sclerosis Society. We thank Patrick Weber for expert technical assistance.

Author contributions

Conception and design of study: C.W.K., S.F. and J.D.L.

Acquisition and analysis of data: C.W.K., M.L., S.E., I.Q., R.T., S.F. and J.D.L.

Valuable discussion/Scientific insight: G.D.L., C.M., M.G.

Providing of materials: G.D.L., S.F., C.M.

Drafting of the manuscript and figures: C.W.K., M.L., G.D.L., S.F., C.M. and J.D.L.

Conflict of interest statement: The authors have declared that no financial conflict of interest exists.

References

1. Bendelac A, Savage PB, Teyton L. The biology of NKT cells. Annu Rev Immunol 2007; 25:297–336.

2. Van Kaer L, Parekh VV, Wu L. Invariant natural killer T cells as sensors and managers of inflammation. Trends in Immunology 2013; 34:50–8.

3. Fujii S-I, Shimizu K, Smith C, Bonifaz L, Steinman RM. Activation of natural killer T cells by alpha-galactosylceramide rapidly induces the full maturation of dendritic cells in vivo and thereby acts as an adjuvant for combined CD4 and CD8 T cell immunity to a coadministered protein. J Exp Med 2003; 198:267–79.

4. Galli G, Pittoni P, Tonti E, Malzone C, Uematsu Y, Tortoli M, Maione D, Volpini G, Finco O, Nuti S, et al. Invariant NKT cells sustain specific B cell responses and memory. Proceedings of the National Academy of Sciences 2007; 104:3984–9.

5. Guillonneau C, Mintern JD, Hubert F-X, Hurt AC, Besra GS, Porcelli S, Barr IG, Doherty PC, Godfrey DI, Turner SJ. Combined NKT cell activation and influenza virus vaccination boosts memory CTL generation and protective immunity. Proc Natl Acad Sci USA 2009; 106:3330–5.

6. Salio M, Silk JD, Jones EY, Cerundolo V. Biology of CD1- and MR1-restricted T cells. Annu Rev Immunol 2014; 32:323–66.

7. Jayawardena-Wolf J, Benlagha K, Chiu YH, Mehr R, Bendelac A. CD1d endosomal trafficking is independently regulated by an intrinsic CD1d-encoded tyrosine motif and by the invariant chain. Immunity 2001; 15:897–908.

8. Kang S-J, Cresswell P. Regulation of intracellular trafficking of human CD1d by association with MHC class II molecules. EMBO J 2002; 21:1650–60.

9. Sugita M, van Der Wel N, Rogers RA, Peters PJ, Brenner MB. CD1c molecules broadly survey the endocytic system. Proceedings of the National Academy of Sciences 2000; 97:8445–50.

10. Chow A, Toomre D, Garrett W, Mellman I. Dendritic cell maturation triggers retrograde MHC class II transport from lysosomes to the plasma membrane. Nature 2002; 418:988–94.

11. Schmid D, Pypaert M, Münz C. Antigen-loading compartments for major histocompatibility complex class II molecules continuously receive input from autophagosomes. Immunity 2007; 26:79–92.

12. Lee HK, Mattei LM, Steinberg BE, Alberts P, Lee YH, Chervonsky A, Mizushima N, Grinstein S, Iwasaki A. In vivo requirement for Atg5 in antigen presentation by dendritic cells. Immunity 2010; 32:227–39.

13. Romao S, Gasser N, Becker AC, Guhl B, Bajagic M, Vanoaica D, Ziegler U, Roesler J, Dengjel J, Reichenbach J, et al. Autophagy proteins stabilize pathogen-containing phagosomes for prolonged MHC II antigen processing. J Cell Biol 2013; 203:757–66.

14. Martinez J, Malireddi RKS, Lu Q, Cunha LD, Pelletier S, Gingras S, Orchard R, Guan J-L, Tan H, Peng J, et al. Molecular characterization of LC3-associated phagocytosis reveals distinct roles for

Rubicon, NOX2 and autophagy proteins. Nature Cell Biology 2015; 17:893–906.

15. Paget C, Mallevaey T, Speak AO, Torres D, Fontaine J, Sheehan KCF, Capron M, Ryffel B, Faveeuw C, Leite de Moraes M, et al. Activation of invariant NKT cells by toll-like receptor 9-stimulated dendritic cells requires type I interferon and charged glycosphingolipids. Immunity 2007; 27:597–609.

16. Lee HK, Mattei LM, Steinberg BE, Alberts P, Lee YH, Chervonsky A, Mizushima N, Grinstein S, Iwasaki A. In Vivo Requirement for Atg5 in Antigen Presentation by Dendritic Cells. Immunity 2010; 32:227–39.

17. Ma J, Becker C, Lowell CA, Underhill DM. Dectin-1-triggered recruitment of light chain 3 protein to phagosomes facilitates major histocompatibility complex class II presentation of fungal-derived antigens. J Biol Chem 2012; 287:34149–56.

18. Freigang S, Landais E, Zadorozhny V, Kain L, Yoshida K, Liu Y, Deng S, Palinski W, Savage PB, Bendelac A, et al. Scavenger receptors target glycolipids for natural killer T cell activation. Journal of Clinical Investigation 2012; 122:3943–54.

19. van den Elzen P, Garg S, León L, Brigl M, Leadbetter EA, Gumperz JE, Dascher CC, Cheng T-Y, Sacks FM, Illarionov PA, et al. Apolipoprotein-mediated pathways of lipid antigen presentation. Nature 2005; 437:906–10.

20. Salio M, Puleston DJ, Mathan TSM, Shepherd D, Stranks AJ, Adamopoulou E, Veerapen N, Besra GS, Hollander GA, Simon AK, et al. Essential role for autophagy during invariant NKT cell development. Proc Natl Acad Sci USA 2014; 111:E5678–87.

21. Inaba K, Inaba M, Romani N, Aya H, Deguchi M, Ikehara S, Muramatsu S, Steinman RM. Generation of large numbers of dendritic cells from mouse bone marrow cultures supplemented with granulocyte/macrophage colony-stimulating factor. J Exp Med 1992; 176:1693–702.

22. Helft J, Böttcher J, Chakravarty P, Zelenay S, Huotari J, Schraml BU, Goubau D, Reis E Sousa C. GM-CSF Mouse Bone Marrow Cultures Comprise a Heterogeneous Population of CD11c(+)MHCII(+) Macrophages and Dendritic Cells. Immunity 2015; 42:1197–211.

23. Guilliams M, Malissen B. A Death Notice for In-Vitro-Generated GM-CSF Dendritic Cells? Immunity 2015; 42:988–90.

24. Kitamura H, Iwakabe K, Yahata T, Nishimura S, Ohta A, Ohmi Y, Sato M, Takeda K, Okumura K, Van Kaer L, et al. The natural killer T (NKT) cell ligand alpha-galactosylceramide demonstrates its immunopotentiating effect by inducing interleukin (IL)-12 production by dendritic cells and IL-12 receptor expression on NKT cells. J Exp Med 1999; 189:1121–8.

25. Yu KOA, Im JS, Illarionov PA, Ndonye RM, Howell AR, Besra GS, Porcelli SA. Production and characterization of monoclonal antibodies against complexes of the NKT cell ligand alpha-galactosylceramide bound to mouse CD1d. J Immunol Methods 2007; 323:11–23.

26. Sugita M, Cernadas M, Brenner MB. New insights into pathways for CD1-mediated antigen presentation. Curr Opin Immunol 2004; 16:90–5.

27. Jayawardena-Wolf J, Bendelac A. CD1 and lipid antigens: intracellular pathways for antigen

presentation. Curr Opin Immunol 2001; 13:109–13.

28. Chiu Y-H, Park S-H, Benlagha K, Forestier C, Jayawardena-Wolf J, Savage PB, Teyton L, Bendelac A. Multiple defects in antigen presentation and T cell development by mice expressing cytoplasmic tail-truncated CD1d. Nat Immunol 2002; 3:55–60.

29. Sugita M, Cao X, Watts GFM, Rogers RA, Bonifacino JS, Brenner MB. Failure of trafficking and antigen presentation by CD1 in AP-3-deficient cells. Immunity 2002; 16:697–706.

30. Elewaut D, Lawton AP, Nagarajan NA, Maverakis E, Khurana A, Honing S, Benedict CA, Sercarz E, Bakke O, Kronenberg M, et al. The Adaptor Protein AP-3 Is Required for CD1d-Mediated Antigen Presentation of Glycosphingolipids and Development of V 14i NKT Cells. Journal of Experimental Medicine 2003; 198:1133–46.

31. Lawton AP, Prigozy TI, Brossay L, Pei B, Khurana A, Martin D, Zhu T, Späte K, Ozga M, Höning S, et al. The mouse CD1d cytoplasmic tail mediates CD1d trafficking and antigen presentation by adaptor protein 3-dependent and -independent mechanisms. J Immunol 2005; 174:3179–86.

32. Noda NN, Ohsumi Y, Inagaki F. Atg8-family interacting motif crucial for selective autophagy. FEBS Lett 2010; 584:1379–85.

33. Pankiv S, Clausen TH, Lamark T, Brech A, Bruun J-A, Outzen H, Øvervatn A, Bjørkøy G, Johansen T. p62/SQSTM1 binds directly to Atg8/LC3 to facilitate degradation of ubiquitinated protein aggregates by autophagy. Journal of Biological Chemistry 2007; 282:24131–45.

34. Tian Y, Chang JC, Fan EY, Flajolet M, Greengard P. Adaptor complex AP2/PICALM, through interaction with LC3, targets Alzheimer's APP-CTF for terminal degradation via autophagy. Proc Natl Acad Sci USA 2013; 110:17071–6.

35. Wilson MT, Johansson C, Olivares-Villagómez D, Singh AK, Stanic AK, Wang C-R, Joyce S, Wick MJ, Van Kaer L. The response of natural killer T cells to glycolipid antigens is characterized by surface receptor down-modulation and expansion. Proceedings of the National Academy of Sciences 2003; 100:10913–8.

36. Ryan MP, Adley CC. Sphingomonas paucimobilis: a persistent Gram-negative nosocomial infectious organism. J Hosp Infect 2010; 75:153–7.

37. Kinjo Y, Wu D, Kim G, Xing G-W, Poles MA, Ho DD, Tsuji M, Kawahara K, Wong C-H, Kronenberg M. Recognition of bacterial glycosphingolipids by natural killer T cells. Nature 2005; 434:520–5.

38. Sriram V, Du W, Gervay-Hague J, Brutkiewicz RR. Cell wall glycosphingolipids of Sphingomonas paucimobilis are CD1d-specific ligands for NKT cells. Eur J Immunol 2005; 35:1692–701.

39. Holzapfel KL, Tyznik AJ, Kronenberg M, Hogquist KA. Antigen-dependent versus -independent activation of invariant NKT cells during infection. The Journal of Immunology 2014; 192:5490–8.

40. Mattner J, Debord KL, Ismail N, Goff RD, Cantu C, Zhou D, Saint-Mezard P, Wang V, Gao Y, Yin N, et al. Exogenous and endogenous glycolipid antigens activate NKT cells during microbial

infections. Nature 2005; 434:525–9.

41. Kinjo Y, Pei B, Bufali S, Raju R, Richardson SK, Imamura M, Fujio M, Wu D, Khurana A, Kawahara K, et al. Natural Sphingomonas glycolipids vary greatly in their ability to activate natural killer T cells. Chem Biol 2008; 15:654–64.

42. Marzo AL, Kinnear BF, Lake RA, Frelinger JJ, Collins EJ, Robinson BW, Scott B. Tumor-specific CD4+ T cells have a major "post-licensing" role in CTL mediated anti-tumor immunity. J Immunol 2000; 165:6047–55.

43. Berner V, Liu H, Zhou Q, Alderson KL, Sun K, Weiss JM, Back TC, Longo DL, Blazar BR, Wiltrout RH, et al. IFN-gamma mediates CD4+ T-cell loss and impairs secondary antitumor responses after successful initial immunotherapy. Nat Med 2007; 13:354–60.

44. Jagannath C, Lindsey DR, Dhandayuthapani S, Xu Y, Hunter RL, Eissa NT. Autophagy enhances the efficacy of BCG vaccine by increasing peptide presentation in mouse dendritic cells. Nat Med 2009; 15:267–76.

45. Ravindran R, Khan N, Nakaya HI, Li S, Loebbermann J, Maddur MS, Park Y, Jones DP, Chappert P, Davoust J, et al. Vaccine activation of the nutrient sensor GCN2 in dendritic cells enhances antigen presentation. Science 2014; 343:313–7.

46. Paludan C, Schmid D, Landthaler M, Vockerodt M, Kube D, Tuschl T, Münz C. Endogenous MHC class II processing of a viral nuclear antigen after autophagy. Science 2005; 307:593–6.

47. English L, Chemali M, Duron J, Rondeau C, Laplante A, Gingras D, Alexander D, Leib D, Norbury C, Lippé R, et al. Autophagy enhances the presentation of endogenous viral antigens on MHC class I molecules during HSV-1 infection. Nat Immunol 2009; 10:480–7.

48. Tey S-K, Khanna R. Autophagy mediates transporter associated with antigen processing-independent presentation of viral epitopes through MHC class I pathway. Blood 2012; 120:994–1004.

49. Sugita M, Grant EP, van Donselaar E, Hsu VW, Rogers RA, Peters PJ, Brenner MB. Separate pathways for antigen presentation by CD1 molecules. Immunity 1999; 11:743–52.

50. Chiu YH, Jayawardena J, Weiss A, Lee D, Park SH, Dautry-Varsat A, Bendelac A. Distinct subsets of CD1d-restricted T cells recognize self-antigens loaded in different cellular compartments. J Exp Med 1999; 189:103–10.

51. Roberts TJ, Sriram V, Spence PM, Gui M, Hayakawa K, Bacik I, Bennink JR, Yewdell JW, Brutkiewicz RR. Recycling CD1d1 molecules present endogenous antigens processed in an endocytic compartment to NKT cells. J Immunol 2002; 168:5409–14.

52. Loi M, Müller A, Steinbach K, Niven J, Barreira da Silva R, Paul P, Ligeon L-A, Caruso A, Albrecht RA, Becker AC, et al. Macroautophagy Proteins Control MHC Class I Levels on Dendritic Cells and Shape Anti-viral CD8(+) T Cell Responses. CellReports 2016; 15:1076–87.

53. Gupta-Rossi N, Ortica S, Meas-Yedid V, Heuss S, Moretti J, Olivo-Marin J-C, Israël A. The adaptor-associated kinase 1, AAK1, is a positive regulator of the Notch pathway. J Biol Chem 2011; 286:18720–30.

54. Henderson DM, Conner SD. A novel AAK1 splice variant functions at multiple steps of the endocytic pathway. Mol Biol Cell 2007; 18:2698–706.

55. Rogov V, Dötsch V, Johansen T, Kirkin V. Interactions between autophagy receptors and ubiquitin-like proteins form the molecular basis for selective autophagy. Mol Cell 2014; 53:167–78.

56. Pei B, Zhao M, Miller BC, Véla JL, Bruinsma MW, Virgin HW, Kronenberg M. Invariant NKT cells require autophagy to coordinate proliferation and survival signals during differentiation. The Journal of Immunology 2015; 194:5872–84.

57. Hara T, Nakamura K, Matsui M, Yamamoto A, Nakahara Y, Suzuki-Migishima R, Yokoyama M, Mishima K, Saito I, Okano H, et al. Suppression of basal autophagy in neural cells causes neurodegenerative disease in mice. Nature 2006; 441:885–9.

58. Schümann J, Facciotti F, Panza L, Michieletti M, Compostella F, Collmann A, Mori L, De Libero G. Differential alteration of lipid antigen presentation to NKT cells due to imbalances in lipid metabolism. Eur J Immunol 2007; 37:1431–41.

Figure Legends

Figure 1

Loss of *Atg5* increases the iNKT cell stimulatory capacity of dendritic cells. C57BL/6 derived splenic DCs were either incubated with 2 μg/ml CpG or left untreated. Original magnification with 63×, 1.4 NA oil immersion lens. Scatter dot plot representation and quantification of colocalization between CD1d and LC3 (Pearson's coefficient analysis). Each symbol represents one cell. Pooled data of 3 independent experiments are shown. Scale bar: 2.5 µm. Statistics: two-tailed Mann-Whitney U Test **(A)**. FACS-sorted CD11c^{+}/I-A^{b+} splenic DCs derived from Cre^{-} *Atg5$^{f/f}$* or Cre^{+} *Atg5$^{f/f}$* animals were pulsed with increasing concentrations of αGalCer or left untreated and subsequently cocultured with the iNKT hybridoma cell line A.407 **(B)** or FF13 (**C**) for 24 hours. IL2 concentration in cell culture supernatants was measured via ELISA. Pooled data and SEM of >3 independent experiments are shown. Each experiment contained at least 3 animals per group. Statistics: Unpaired two-tailed T test. C57BL/6 derived purified splenic DCs were treated with rapamycin (RAP; 12.5 µM; 4 hours), subsequently pulsed with αGalCer (1 μg/ml; 4 hours) and cocultured with iNKT hybridoma cell line A.407 (24 hours). IL2 concentration in cell culture supernatants was measured via ELISA. Pooled data and SEM of 3 independent experiments is shown. Each experiment contained at least 3 animals per group. Statistics: Unpaired two-tailed T test **(D)**. *** $p \leq 0.001$,** $p \leq 0.01$,* ≤ 0.05, ns $p > 0.05$.

Figure 2

Receptor-mediated uptake of glycolipid antigens and costimulatory properties remain unchanged in Cre^{+} *Atg5$^{f/f}$* DCs. CD1d-presentation of indicated iNKT cell agonists by primary splenic DCs was assessed using activation of the iNKT hybridoma A.407 as in Fig. 1B **(A)**. Splenic DCs derived from either Cre^{-} *Atg5$^{f/f}$* or Cre^{+} *Atg5$^{f/f}$* animals were stained for CD40 surface expression. Pooled data and SEM of 3 independent experiments are shown. Each experiment contained at least 3 animals per group. Statistics: Unpaired two-tailed T test **(B)**. Frequency of IL12-producing splenic DCs upon CD40 ligation. Purified splenic DCs were either incubated with anti-CD40 overnight or left untreated. IL12 production was measured via intracellular cytokine staining and by ELISA. Results of 3 independent experiments are shown. Each experiment contained at least 3 animals per group. Statistics: Unpaired two-tailed T test **(C)**. *** $p \leq 0.001$,** $p \leq 0.01$,* ≤ 0.05, ns $p > 0.05$.

Figure 3

Increased CD1d surface expression in Cre$^+$ *Atg5$^{f/f}$* DCs. Flow cytometric analysis of CD1d surface levels on splenic DCs. Representative contour plots of splenic DCs or B cells and histograms showing CD1d surface expression **(A)**. Quantification of CD1d surface expression on splenic DCs and B cells. Pooled data and SEM from >3 independent experiments are shown. Each experiment contained at least 2 animals per group. Statistics: Unpaired two-tailed T test **(B)**. CD1d: αGalCer-complex staining (L363 clone) in splenic DCs or B cells 4 hours after i.p. application of either αGalCer or PBS. Pooled data and SEM from 2 independent experiments is shown. Statistics: Unpaired two-tailed T test **(C)**. DC surface expression of CD11c or I-A^b. Pooled data and SEM from >3 independent experiments is shown. Each experiment contained at least 2 animals per group. Statistics: Unpaired two-tailed T test **(D)**. *** $p \leq 0.001$,** $p \leq 0.01$,* ≤ 0.05, ns $p > 0.05$.

Figure 4

Impaired CD1d internalization in Cre$^+$ *Atg5$^{f/f}$* DCs. CD1d surface levels are determined by the rates of CD1d internalization and recycling through endosomal and lysosomal compartments **(A)**. Internalization of surface CD1d on splenic DCs or splenic B cells was analyzed using a biotin-based flow cytometric endocytosis assay. Pooled data and SEM of at least 3 independent experiments are shown. Each experiment contained at least 2 animals per group. Statistics: Unpaired two-tailed T test **(B)**. CD1d recycling in splenic DCs or splenic B cells was analyzed using a flow cytometry based recycling assay. Pooled data and SEM of at least 3 independent experiments are shown. Each experiment contained at least 2 animals per group. Statistics: Unpaired two-tailed T test **(C)**. Colocalization study of AP2/EEA1 and CD1d/EEA1 via confocal microscopy. Original magnification with 63 ×, 1.4 NA oil immersion lens. Representative photographs from 2 independent experiments per colocalization study are shown. Scale bar: 2.5 µm **(D)**. Scatter dot plot representation and quantification of colocalization between AP2/EEA1 and between CD1/EEA1 via Pearson's coefficient. Each symbol represents one cell. Pooled data of 2 independent experiments per colocalization study are shown. Statistics: Unpaired two-tailed T test **(E)**. *** $p \leq 0.001$,** $p \leq 0.01$,* ≤ 0.05, ns $p > 0.05$.

Figure 5

Autophagy proteins in DCs regulate iNKT cell responses to lipid immunization and microbial infection *in vivo.* Frequencies of iNKT cells (thymus, spleen and liver) from naïve Cre^{-} *Atg5*$^{f/f}$ and Cre^{+} *Atg5*$^{f/f}$ mice were quantified. Representative dot plots from at least two independent experiments are shown **(A)**. Serum concentration kinetics of IL4 and IFNG upon glycolipid challenge *in vivo* measured via ELISA **(B)**. Surface expression kinetics of CD86 and CD40 on splenic DCs. Each symbol represents one animal. Pooled data of at least 2 independent experiments are shown. Statistics: Unpaired two-tailed T test **(C)**. Quantification of bacterial titers (CFU/ g tissue) in spleen and lung after *in vivo* infection of mice with *S. paucimobilis*. Each symbol represents one animal. One representative of two experiments with similar results is shown. Quantification of serum cytokines upon *in vivo* infection with *S. paucimobilis.* One representative of two experiments with similar results is shown. Statistics: two-tailed Mann-Whitney U Test **(D)**. *** $p \leq 0.001$,** $p \leq 0.01$,* ≤ 0.05, ns $p > 0.05$.

Figure 1

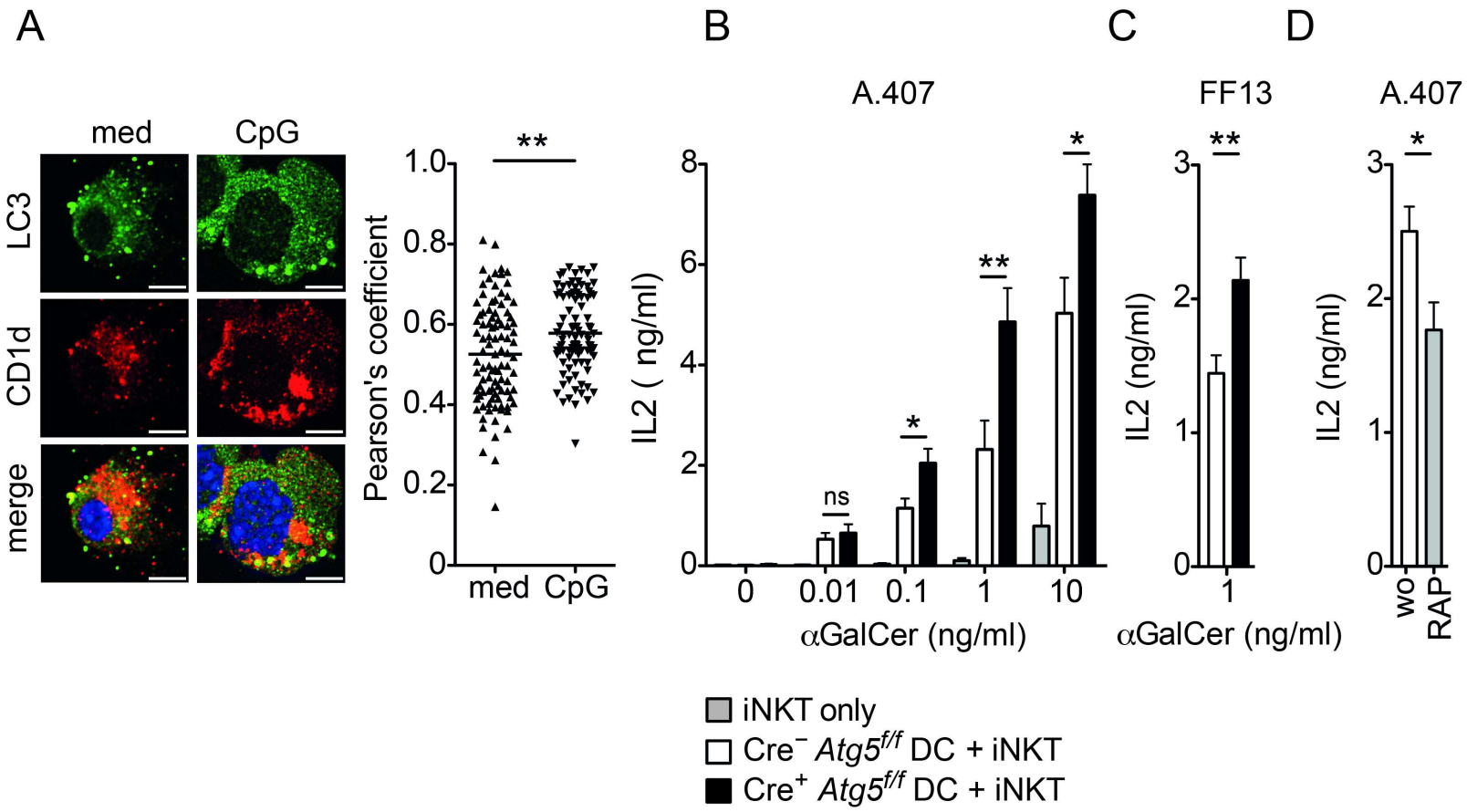
A
med
CpG
LC3
CD1d
merge
Pearson's coefficient
1.0
0.8
0.6
0.4
0.2
0
**
med
CpG
B
A.407
IL2 (ng/ml)
8
6
4
2
0
ns
*
**
*
0
0.01
0.1
1
10
αGalCer (ng/ml)
C
FF13
IL2 (ng/ml)
3
2
1
0
**
1
αGalCer (ng/ml)
D
A.407
IL2 (ng/ml)
3
2
1
0
*
wo
RAP
iNKT only
Cre⁻ Atg5f/f DC + iNKT
Cre+ Atg5f/f DC + iNKT

Figure 2

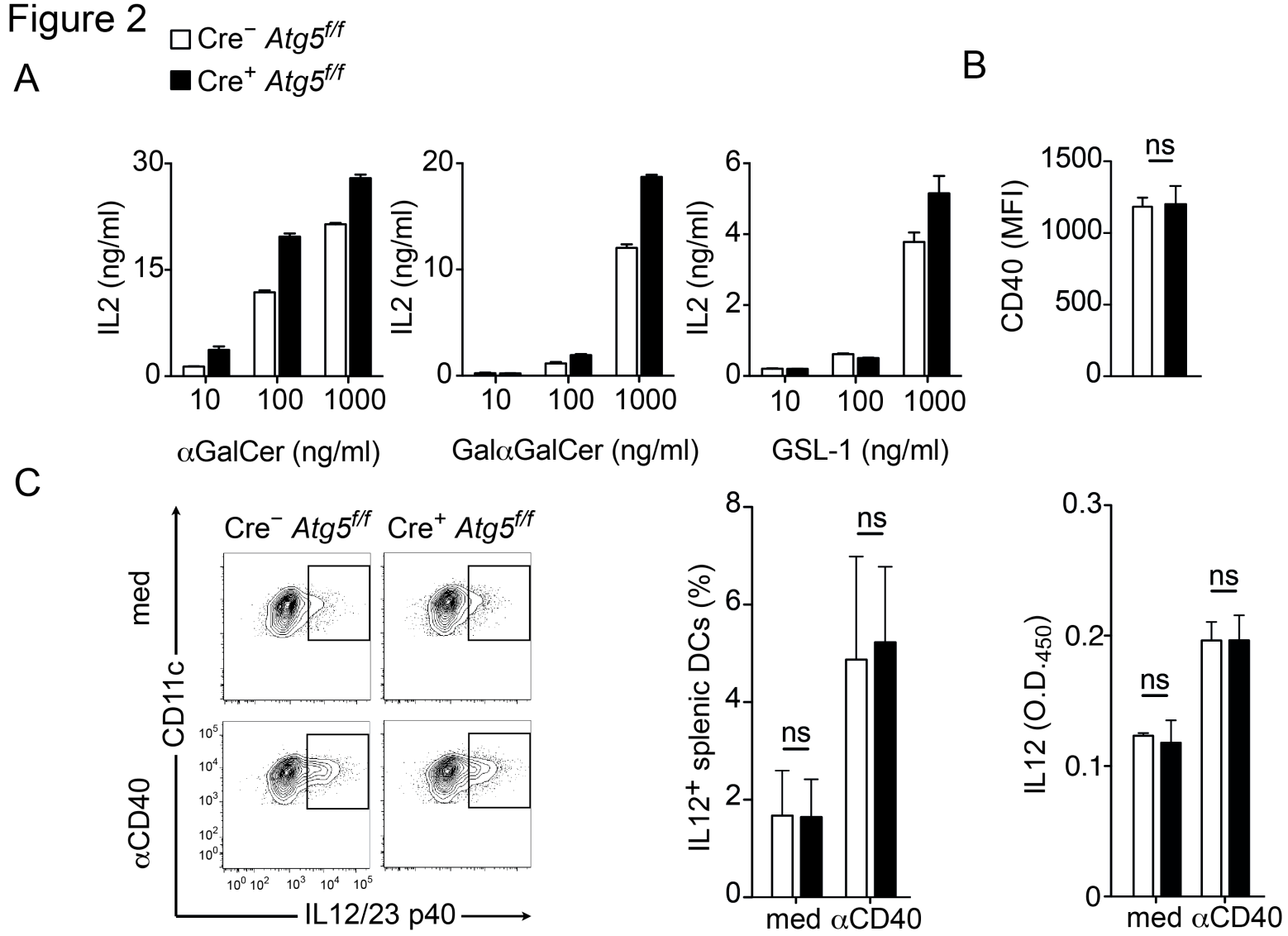
A
Cre⁻ Atg5f/f
Cre+ Atg5f/f
IL2 (ng/ml)
αGalCer (ng/ml)
GalαGalCer (ng/ml)
GSL-1 (ng/ml)
B
CD40 (MFI)
ns
C
Cre⁻ Atg5f/f
Cre+ Atg5f/f
med
αCD40
CD11c
IL12/23 p40
IL12+ splenic DCs (%)
IL12 (O.D.450)
med
αCD40

Figure 3

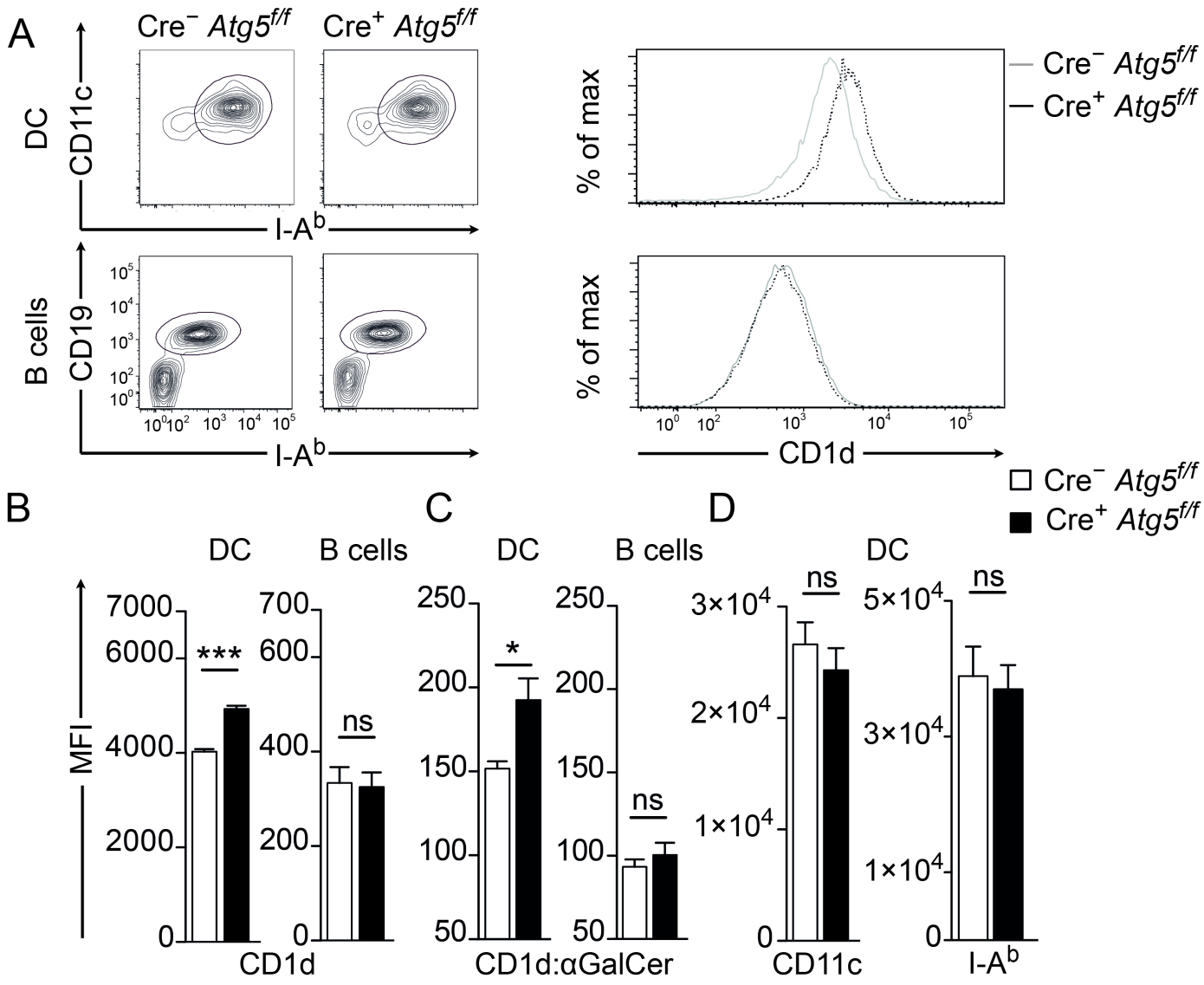
A
Cre⁻ Atg5f/f
Cre+ Atg5f/f
DC
CD11c
I-Ab
B cells
CD19
% of max
CD1d
B
C
D
MFI
***
ns
*
CD1d
CD1d:αGalCer
CD11c
I-Ab

Figure 4

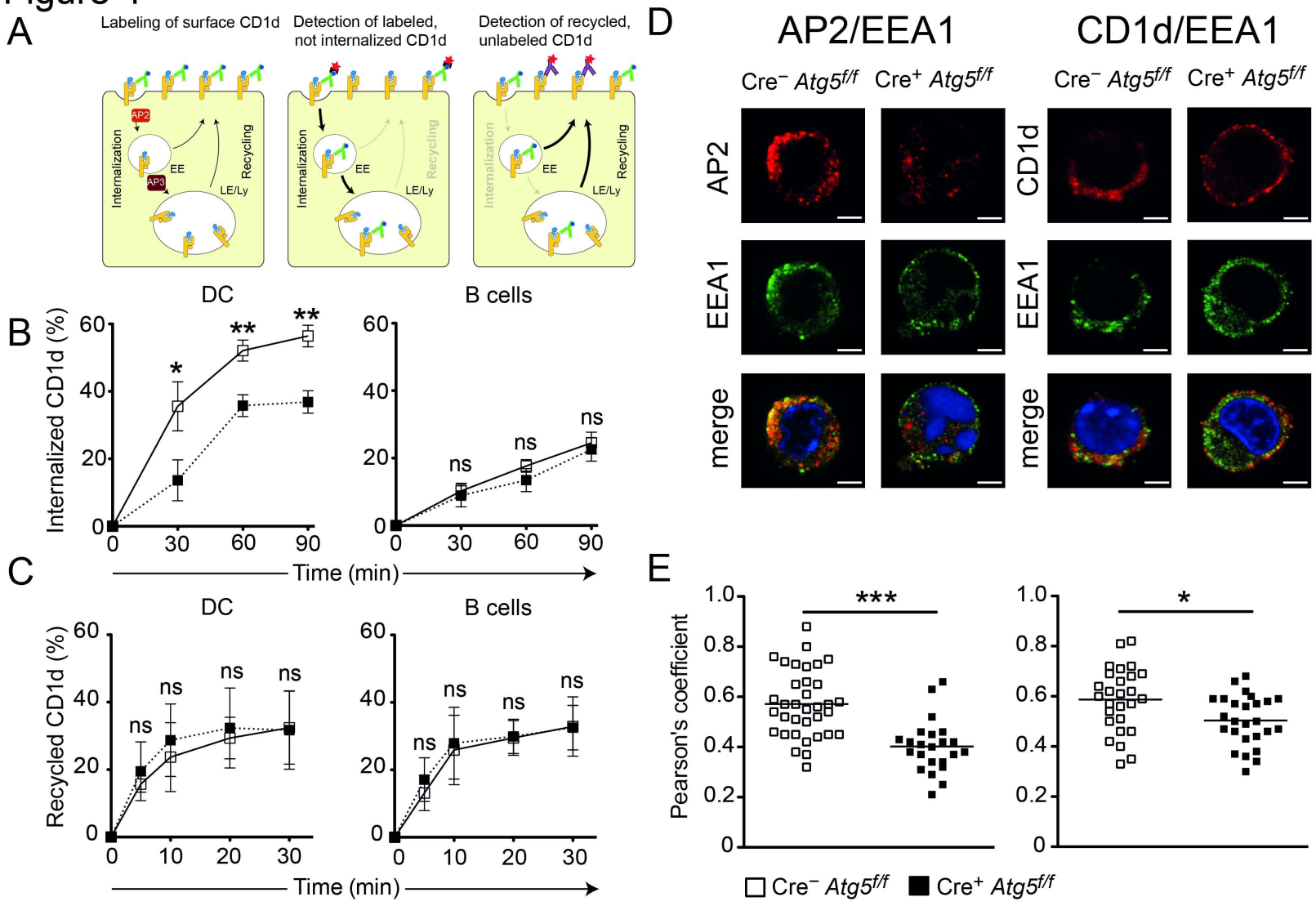
A
Labeling of surface CD1d
Detection of labeled, not internalized CD1d
Detection of recycled, unlabeled CD1d
AP2
AP3
EE
LE/Ly
Internalization
Recycling
B
DC
B cells
Internalized CD1d (%)
Time (min)
C
Recycled CD1d (%)
ns
D
AP2/EEA1
CD1d/EEA1
Cre⁻ Atg5f/f
Cre⁺ Atg5f/f
AP2
CD1d
EEA1
merge
E
Pearson's coefficient
***
*

Figure 5

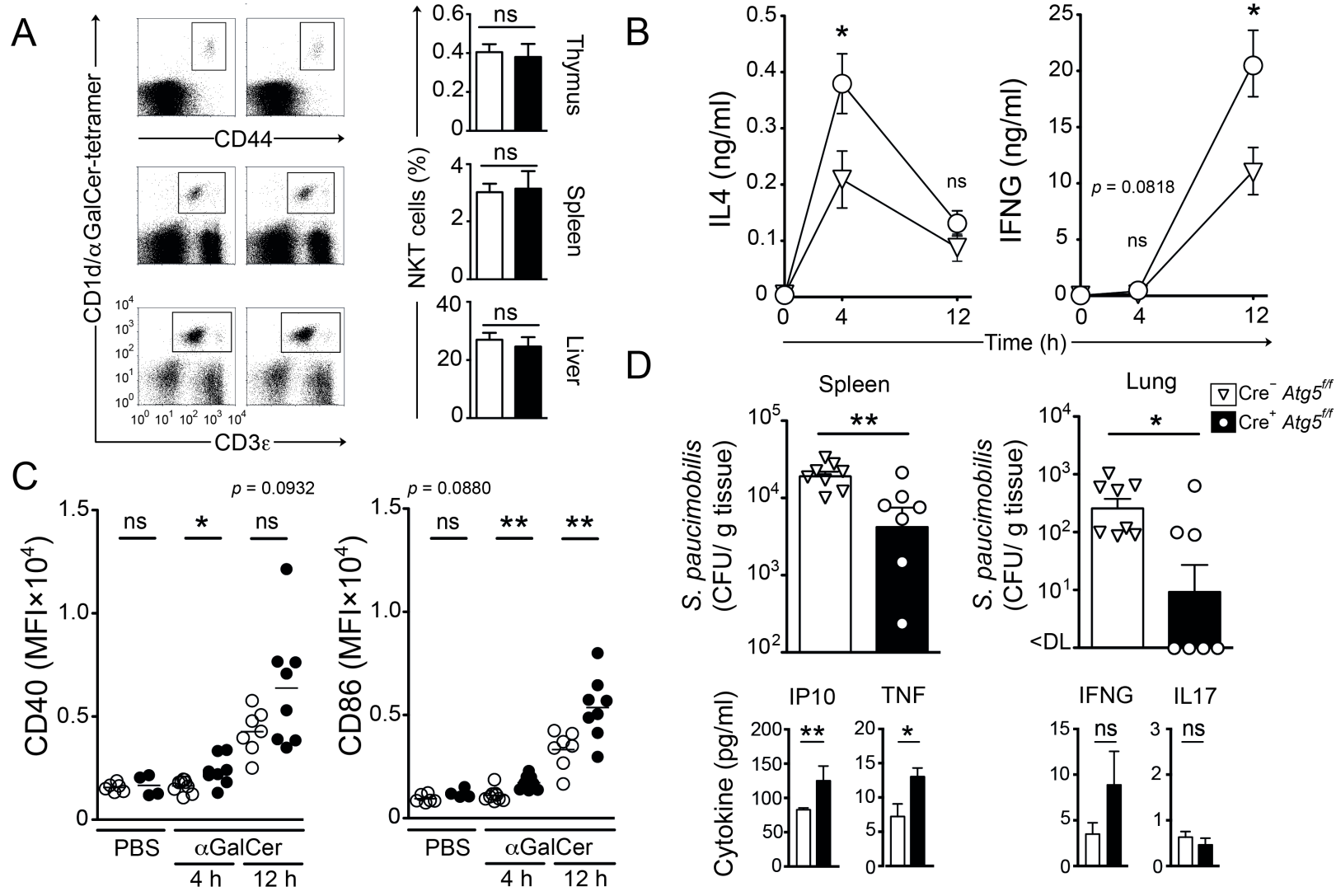
A
CD1d/αGalCer-tetramer
CD44
CD3ε
NKT cells (%)
Thymus
Spleen
Liver
ns
B
IL4 (ng/ml)
IFNG (ng/ml)
p = 0.0818
Time (h)
C
CD40 (MFI×10^4)
CD86 (MFI×10^4)
p = 0.0932
p = 0.0880
PBS
αGalCer
4 h
12 h
D
Spleen
Lung
S. paucimobilis (CFU/ g tissue)
Cre⁻ Atg5f/f
Cre⁺ Atg5f/f
<DL
Cytokine (pg/ml)
IP10
TNF
IFNG
IL17